

FedUHD: Unsupervised Federated Learning using Hyperdimensional Computing

You Hak Lee, Xiaofan Yu, Quanling Zhao, Flavio Ponzina, and Tajana Rosing

University of California San Diego, USA

{yhl004, x1yu, quzhao, fponzina, tajana}@ucsd.edu

Abstract—Unsupervised federated learning (UFL) has gained attention as a privacy-preserving, decentralized machine learning approach that eliminates the need for labor-intensive data labeling. However, UFL faces several challenges in practical applications: (1) non-independent and identically distributed (non-iid) data distribution across devices, (2) expensive computational and communication costs at the edge, and (3) vulnerability to communication noise. Previous UFL approaches have relied on deep neural networks (NN), which introduce substantial overhead in both computation and communication. In this paper, we propose FedUHD, the first UFL framework based on Hyperdimensional Computing (HDC). HDC is a brain-inspired computing scheme with lightweight training and inference operations, much smaller model size, and robustness to communication noise. FedUHD introduces two novel HDC-based designs to improve UFL performance. On the client side, a kNN-based cluster hypervector removal method addresses non-iid data samples by eliminating detrimental outliers. On the server side, a weighted HDC aggregation technique balances the non-iid data distribution across clients. Our experiments demonstrate that FedUHD achieves up to $173.6\times$ and $612.7\times$ better speedup and energy efficiency, respectively, in training, up to $271\times$ lower communication cost, and 15.50% higher accuracy on average across diverse settings, along with superior robustness to various types of noise compared to state-of-the-art NN-based UFL approaches.

Index Terms—Unsupervised Learning, Federated Learning, Hyperdimensional Computing, edge AI

I. INTRODUCTION

The rapid proliferation of connected devices has resulted in a massive volume of data generated at the edge. This phenomenon has underscored the importance of federated learning (FL), a decentralized machine learning paradigm. FL has emerged as a crucial research particularly in privacy-sensitive domains such as surveillance systems [1] and face recognition [2]. FL training has two core components: a central server and a set of client devices. Each client trains a model locally on its own privacy-sensitive data and then sends only the resulting trained model to the server, thereby avoiding the need to share raw data. The server then gathers the locally trained models and aggregates them to obtain a new global model. Finally, the server distributes the updated model back to the clients. This process of communication between the clients and the server continues for a pre-defined number of rounds until the convergence.

Although FL has shown significant promise, most research so far has focused on supervised settings that assume all local data is labeled. Such an assumption can be unrealistic as labeling requires human intervention and is usually costly [3].

Accordingly, the demand for unsupervised federated learning (UFL) has increased [3]–[6].

However, unsupervised FL encounters various challenges in real-world deployments: (1) The presence of non-independent and identically distributed (non-iid) and unlabeled data across devices. In a non-iid data setting, the globally aggregated information can be unrepresentative or biased [6]. The non-iid challenge is exacerbated in unsupervised FL. (2) Expensive computational and communication costs on the edge. Training an NN model on an edge device presents a crucial computational challenge primarily due to resource-intensive backpropagation operations. Furthermore, an NN model has a substantial number of parameters (e.g., 11.7 million for ResNet18 [7]) that must be communicated between the central server and clients. (3) Vulnerability to communication noise. Given that edge devices often operate in unreliable communication environments, packet loss and random noise are common during data transmission [8]. Under these conditions, the robustness of models trained through UFL becomes a critical factor in overall system performance. Traditional FL methods based on NN models are vulnerable to communication noise [9], [10].

Hyperdimensional computing (HDC) presents a compelling approach to overcoming these challenges. As a brain-inspired computational paradigm, HDC encodes input data into high-dimensional vectors, known as hypervectors (HVs). The growing interest in HDC is attributed to its energy efficiency, which results from lightweight training that does not require backpropagation [11], and its robustness, which arises from the holistic representation (i.e., if an element of an HV flipped, it does not dramatically affect a specific input feature) [10]. HDC has been effectively applied to machine learning tasks, such as image classification [12] and graph node classification [11], and has also been used in FL settings [9], [10]. HDC-based FL is particularly well suited for deployment in edge devices, achieving accuracy comparable to NN-based FL while requiring a smaller model size ($<1/10$) and reduced computational complexity ($<1/100$).

However, existing HDC-based FL approaches are limited to supervised learning. It remains unclear how to enable unsupervised FL with HDC, which heavily relies on labeled data to train class hypervectors. In this paper, we introduce FedUHD, the first framework for unsupervised FL based on HDC. FedUHD resolves the high computation and communication costs as well as the vulnerability to noise with HDC’s inherent properties.

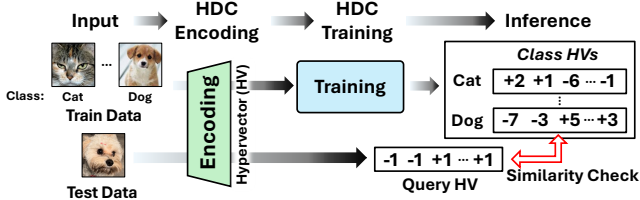


Fig. 1: Overview of the HDC training and inference flow.

Moreover, FedUHD contains two novel designs for clients and the server to tackle the non-iid unlabeled data distribution challenge. On the client side, it employs a kNN-based cluster HV removal method to identify and remove local outliers. On the server side, it uses a weighted HDC aggregation technique to balance the non-iid data distribution among clients.

We comprehensively evaluate FedUHD in non-iid UFL settings. Our results show an average accuracy improvement of 15.50%, up to 173.6 \times and 612.7 \times better speedup and energy efficiency, and up to 271 \times lower communication compared to state-of-the-art NN-based UFL framework [6] across all datasets. Additionally, we evaluate FedUHD under various communication failure scenarios and observe up to 49.27 percent points smaller accuracy degradation, demonstrating superior robustness compared to the state-of-the-art NN-based UFL method [6]. The integration of HDC with the UFL paradigm offers significant potential for enhancing decentralized, privacy-preserving machine learning on edge devices, especially under limited hardware resources and unreliable communication environments.

II. RELATED WORK AND BACKGROUND

A. NN-based Unsupervised Federated Learning

Early FL research has focused on supervised and semi-supervised scenarios, but their performance can degrade significantly when labels are limited [3]. Recently, several studies [3]–[6] have been conducted research in UFL. FedU [3] tackled the degradation of local models due to data heterogeneity by implementing divergence-aware predictor updates. FedUL [4] facilitated the transformation of UFL into a conventional supervised FL framework by introducing temporal labels called surrogate labels. FedX [5] improved the training efficiency and convergence stability in UFL by a two-sided knowledge distillation process between local and global models. Orchestra [6] uses a clustering-based approach for UFL, maintaining local clusters on each client and global clusters in the cloud. However, Orchestra performs well only with easily clusterable representations.

The main issue with existing UFL research is its reliance on NN models. NN models require significant resources to train [13], incur high communication costs, and also exhibit vulnerability to various communication noises such as packet loss [9], [10]. FedUHD addresses all three challenges by incorporating HDC.

B. HDC Background

Hyperdimensional Computing is an emerging computing paradigm for solving cognitive information processing tasks

with data represented as high-dimensional and often low-precision vectors, “hypervectors (HVs)” [14], [15]. Learning in HDC is achieved through simple and parallelizable operations using hypervectors, such as element-wise addition and multiplication [16], [17]. HDC has been widely applied in a variety of machine learning problems, such as classification [16] and regression [18]. The popularity of HDC stems from two key advantages. First, HDC transforms non-separable patterns in the original space into linearly separable ones in the high-dimensional space. Second, its lightweight learning operations offer superior memory efficiency and faster training compared to traditional machine learning approaches such as deep learning [19].

The first stage of any HDC learning algorithm is encoding, which maps the data from its ambient representation to HVs. There are several approaches in HDC literature for encoding functions that preserve different types of similarity, such as linear random projection [20] and Random Fourier Features [21]. After encoding, learning with HVs is straightforward: data HVs from the same category are bundled (e.g., via element-wise addition) to form a single class HV that aggregates class-specific information. Classification and inference are then performed through a similarity search between query HVs and class HVs, typically using metrics like Hamming distance or cosine similarity. In multi-epoch settings, class HVs are often fine-tuned using the perceptron algorithm [22], where misclassified samples are removed from the incorrect class HV and added to the correct one.

C. HDC and Federated Learning

Recent studies [9], [10], [23], [24] have shown that HDC’s benefits can be effectively applied to FL. Instead of transmitting model weights, lightweight and noise-tolerant class HVs learned on individual clients are exchanged, aggregated through bundling, and redistributed to the clients. This process is repeated for multiple rounds until the global model converges.

FL-HDC [23] reduces communication overhead significantly by transmitting bipolarizing model HVs instead of traditional model weights which requires high precision. RE-FHDC [24] further reduces computational and communication overhead by partitioning HVs during the training and transfer phases. FHDnn [10] integrates pre-trained convolutional neural networks (CNN) with HDC, to combine the capability of DNN and the efficiency of HDC in a federated setting. FedHD [9] demonstrates HDC-based federated learning practically using real edge computing devices and under real network conditions.

Despite the above contributions, these techniques are not applicable in scenarios without label supervision. In contrast, we address UFL using HDC by proposing FedUHD.

III. FEDUHD

FedUHD is the first HDC-based UFL framework more energy efficient and robust than NN-based methods, while removing the reliance on labeled data in comparison to prior HDC-based supervised FL. FedUHD inherits the lightweight operations

Algorithm 1 FedUHD Training Procedure

```

1: Initialize: round index  $rnd \leftarrow 0$ , randomly initialize global centroid
hypervectors  $\mathcal{O}$ 
2: // Local Training at Client  $i$ 
3: Input:
    • HDC dimension  $D$ , number of centroids  $J$ 
    • Feature extractor  $f$ , random projection function  $r$ 
    • Local training data  $\mathcal{X}_i$ , number of local epochs  $E$ 
    • Global centroids from previous round  $\mathcal{G}$ 
4: Step 1: HDC Encoding
5: Initialize empty list  $enc\_H$  to store encoded hypervectors
6: for each input  $\mathbf{x}_{in} \in \mathcal{X}_i$  do
7:   Encode:  $H_{in} \leftarrow r(f(\mathbf{x}_{in}))$  // $f$  is used in case  $\mathbf{x}_{in}$  is an image only
8:   Append  $H_{in}$  to  $enc\_H$ 
9: end for
10: Step 2: Clustering with kNN-based Filtering
11: if  $rnd > 0$  then
12:   For each global centroid in  $\mathcal{G}$ , check whether any  $H_{in} \in enc\_H$ 
       shares the same cluster ID among its  $k_n$  nearest neighbors
13:   Remove centroid from  $\mathcal{G}$  and  $\mathcal{L}_i$  if no match is found
14:   Set  $\mathcal{G}_i \leftarrow$  remaining global centroids (used as initialization)
15: else
16:    $\mathcal{G}_i \leftarrow \mathcal{O}$                                 ▷ Use initial random centroids
17: end if
18: Run local clustering:
19:  $\mathcal{L}_i, cluster\_ids \leftarrow kMeans(enc\_H, iter = E, init = \mathcal{G}_i)$ 
20: Count number of samples per cluster:  $S_{ij}$ 
21: return  $\mathcal{L}_i, S_i = \{S_1, \dots, S_J\}$  ▷ Local centroid HVs and cluster sizes
22: // Global Aggregation
23: Input:
    • Number of clients  $I$ , number of centroids  $J$ 
    • Local centroid HVs  $\mathcal{L}_i$  and cluster sizes  $S_i$  from each client
24: Step 3: Weighted HDC Aggregation
25: for each centroid  $j = 1$  to  $J$  do
26:   Compute weights:  $W_{ij} \leftarrow \frac{S_{ij}}{\sum_{i=1}^I S_{ij}}$ 
27:   Aggregate:  $\mathbf{g}_j \leftarrow \sum_{i=1}^I W_{ij} \cdot \mathbf{l}_{ij}$ 
28: end for
29: Update round index:  $rnd \leftarrow rnd + 1$ 
30: return Updated global centroids  $\mathcal{G} = \{\mathbf{g}_1, \dots, \mathbf{g}_J\}$ 

```

and small model sizes of HDC, thus excels in computational and communication efficiency.

However, a key challenge in HDC-based UFL is effectively training local models with unlabeled non-iid data on local devices and aggregating these models at a central server. The absence of class label information during local training and global aggregation makes it difficult to construct and combine models. This problem is exacerbated in non-iid settings, which increase the discrepancies between local and global models. Model convergence is increasingly challenging under non-iid data distribution without labels [3].

The proposed FedUHD introduces two new techniques to handle non-iid data settings in the absence of labels. First, on the client side, we propose a kNN-based cluster HV removal technique to accept only partial global information that is beneficial for training on each local device. Second, on the server side, we design a weighted HDC aggregation approach to effectively balance the non-iid data distribution among clients even without labels.

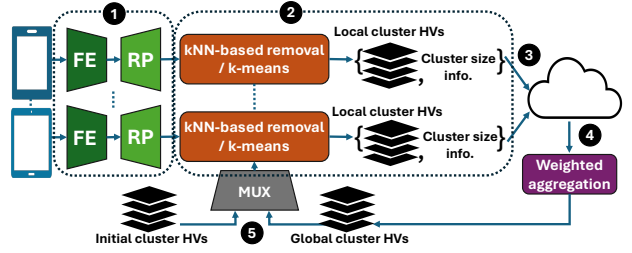


Fig. 2: FedUHD framework overview. FE and RP means feature extraction and random projection, which are standard setup for HDC-based FL [9], [10].

A. Overview of FedUHD

Without ground-truth labels, the objective for FedUHD is to train a set of global cluster HVs, $\mathcal{G} = \{\mathbf{g}_j \in \mathbb{R}^D\}$ where $j \in \{1, \dots, J\}$ and D is HDC dimension. In unsupervised learning, the exact number of classes (labels) K is unknown, so we assume a larger number of centroids or clusters, denoted as J ($J > K$). The total number of clients is I . $\mathcal{X}_i = \{\mathbf{x}_j\}_{j=1}^{n_i}$ represents the local training dataset for client i . Let $n_i = |\mathcal{X}_i|$ denote the number of client i 's data samples and $n = \sum_{i=1}^I n_i$ denote the total data samples of all clients.

To train global cluster HVs, FedUHD is composed of 5 steps as shown in Fig. 2 and Algorithm 1. Training is mainly divided into local training (steps ①-③) and global aggregation (steps ④-⑤).

① **HDC encoding** maps client data into a high-dimensional space. FedUHD uses standard random projection (RP) [14] for simple data and incorporates a shallow pretrained feature extractor (FE) to handle image inputs [25]. Using a pretrained FE is a common practice in HDC pipelines for image processing [9], [10]. The FE remains frozen during both training and inference, ensuring a good balance between classification accuracy and energy efficiency [25]. Once all training data are converted to HVs, the HDC encoding step is completed. We refer to the encoded HVs as enc_H .

② In the local phase, FedUHD **trains local cluster HVs** instead of class HVs due to the lack of labels in unsupervised FL. Unlike existing distributed clustering methods [26] or Orchestra [6], FedUHD performs local k-means clustering on encoded HVs, offering better separability and robustness due to the high dimensionality. Specifically, all clients begin with shared initial cluster HVs randomly generated on the server, each having its own $cluster_id$. The high-dimensional data points to be clustered are in enc_H s from the HDC encoding step. The number of iterations of local clustering is set to the number of local epochs E . After running local clustering, FedUHD designs a novel kNN-based cluster HV removal process (elaborated in Section III-B) to remove outlier global/local cluster HVs resulting from the non-iid data distribution. Subsequently, FedUHD conducts local clustering again with the remaining global cluster HVs as the new initial centroids. Let k_m be the number of clusters for local clustering, initialized as $k_m = J$. k_n is used for the kNN removal process.

③ The final step of the local training is to **send a model to the server**. Unlike NN-based UFL, FedUHD maintains a set of

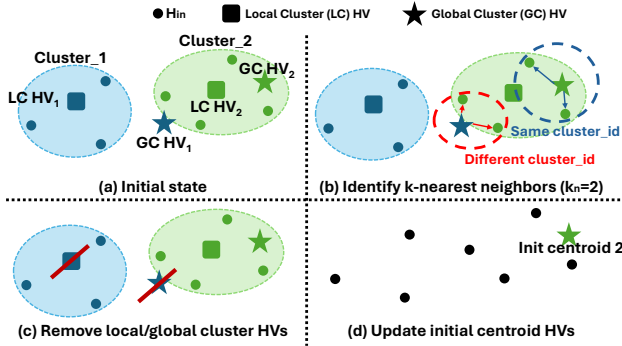


Fig. 3: Visualization of the kNN-based cluster HV removal process.

local cluster HVs (\mathcal{L}_i) as the model. FedUHD also shares the size of each local cluster (S_{ij}) with the cloud, which is obtained by counting the $cluster_id$ of local HV (H_{in}) samples.

④ In the **global aggregation phase**, local models are combined to build a global model using the weighted HDC aggregation method described in Section III-C. Here a set of global cluster HVs is treated as the global model (\mathcal{G}).

⑤ In the **global model transfer stage**, the server sends the global model back to the clients. Before the start of the first communication round ($rnd=0$), a set of initial cluster HVs (\mathcal{O}) is randomly generated and sent to each client. In subsequent rounds, the server sends the latest global model \mathcal{G} resulting from global aggregation.

B. KNN-based Cluster HV Removal on Clients

In non-iid scenarios, local models may become biased toward specific distributions and the aggregated global model misrepresent these local distributions. Consequently, when the global model is sent back to local devices, it may hinder rather than facilitate model convergence. To this end, we introduce a kNN-based cluster hypervector removal technique for FedUHD.

Fig. 3 shows the detailed process of kNN-based cluster HV removal in a simple example. The removal consists of four stages: initial state, identify k-nearest neighbors, remove local and global cluster HVs, and update initial centroid HVs for the current round. Fig. 3 (a) illustrates the state before applying the kNN-based cluster HV removal. As a result of the previous round of local training, two clusters have been formed, with each color representing one $cluster_id$. The individual points represent the H_{in} s, while the squares denote the local cluster HVs from the previous round, and the stars indicate the global cluster HVs received from the server after the global aggregation.

In the “identify k-nearest neighbors” phase (Fig. 3 (b)), each global cluster HV is examined by identifying the $cluster_ids$ of its k_n nearest neighboring H_{in} s, where k_n is a predefined value. Fig. 3 (b) illustrates a case where k_n is set to 2. For Global Cluster HV 1 the nearest H_{in} s all have $cluster_id$ of 2, whereas, for Global Cluster HV 2, the nearest H_{in} s have $cluster_id$ of 2. If, during the “identify k-nearest neighbors” phase, a global cluster HV has no neighboring H_{in} s with the same $cluster_id$, FedUHD treats the global cluster HV as an “outlier” and the corresponding global and local cluster HV of

TABLE I: Detailed experimental setup of FedUHD on various datasets. FCL: fully-connected layer.

	# features	Clients	Method	Baseline
HAR [29]	561	10	HDC	3 FCLs
CIFAR [30]	32x32x3	10/100	FE + HDC	ResNet18

that $cluster_id$ are removed in the “remove local and global HVs” stage for the current round. Fig. 3 (c) shows the removal of Global/Local Cluster HV 1. Finally, the initial centroid HVs for the current round’s local clustering are updated with the remaining global cluster HVs (Fig. 3 (d)). k_{mi} value is adjusted by subtracting the number of $cluster_ids$ removed during the cluster HV removal stage from the previous k_{mi} value.

C. Weighted HDC Aggregation in Cloud

To aggregate local models in a label-free and non-iid data setting across devices, we propose a new weighted HDC aggregation method in the cloud. Unlike HDC-based supervised FL, the lack of labels prevents the direct use of techniques like bundling [10] or FedAvg [27], which are typically employed in global aggregation. Drawing inspiration from weighted k-means [28] and FedAvg, FedUHD assigns weights to local cluster hypervectors for all $cluster_ids$. Let \mathbf{l}_{ij} denote the local cluster HV on client i with $cluster_id$ j , S_{ij} denote the size of cluster j in client i . FedUHD performs weighted HDC aggregation to combine the local models and obtain a new global cluster \mathbf{g}_j as follows:

$$W_{ij} = \frac{S_{ij}}{\sum_{i=1}^I S_{ij}}, \mathbf{g}_j = \sum_{i=1}^I W_{ij} * \mathbf{l}_{ij} \quad (1)$$

By applying weighted HDC aggregation on the server, FedUHD effectively merges local models by considering cluster sizes, even in the absence of labels, resulting in a balanced global model in non-iid data scenarios.

IV. RESULTS

A. Experimental Setup

Datasets: We conduct experiments for various applications including human activity recognition and image classification. We use HAR [29], CIFAR10/100 [30] datasets, the standard datasets for these scenarios. Each sample in the HAR dataset consists of 561 features extracted from IMU sensors, while CIFAR-10/100 comprises 32x32 RGB images. These datasets are distributed across I clients by sampling class priors from a Dirichlet distribution ($Dir(\alpha)$) with α set to 0.1, which is the same setting as the state-of-the-art NN-based UFL [6]. We evaluate typical FL cases with 10 and 100 clients for the CIFAR-10/100 datasets. For the HAR dataset, we only consider the 10-client case due to its limited size. The detailed setup of FedUHD on each dataset is summarized in Table I.

Metrics: We use the unsupervised clustering accuracy metric (ACC) that is commonly used in previous unsupervised learning work [31], [32]. Unlike traditional accuracy metrics and the linear evaluation protocols [5], [6], ACC does not require prior knowledge of the number of classes, nor training a linear classifier with a subset of labeled samples, making it more suitable for unsupervised learning scenarios. Let $\phi(\theta(\mathbf{x}_j))$

denote the predicted cluster labels and y_j the ground-truth labels. ACC is computed as follows:

$$ACC = \max_m \frac{1}{|\mathcal{X}^{test}|} \sum_{j=1}^{|\mathcal{X}^{test}|} \mathbf{1}\{y_j = \phi(\theta(\mathbf{x}_j))\}, \quad (2)$$

where m ranges over all possible one-to-one mappings between predicted clusters and ground-truth classes. Intuitively, ACC measures the accuracy under the “best” mapping between the predicted cluster labels and the true labels. In addition, we examine the training time and energy consumed for end-to-end training. We also evaluate the communication cost for each communication round.

Baselines: We adopt state-of-the-art unsupervised FL frameworks as comparisons, including Orchestra [6] and its baselines (f-BYOL [33], f-specloss [2], f-simsiam [34], f-simclr [35]). These methods are selected for state-of-the-art performances and realistic settings with a large number of clients (up to 400). We exclude FedUL [4], FedU [3], and FedX [5] due to impractical data distributions and small client sets. We use a ResNet18 backbone [36] as the baseline model for CIFAR10/100. For HAR, we use a simple NN model with three fully connected layers of 512 units each, following previous work [6], [37]. We use the original hyperparameter settings from the Orchestra codebase.

Implementation Details: We implement FedUHD with Python-based libraries [38], [39]. We use the standard random projection HDC encoding for HAR workloads [14]. For CIFAR10/100, we use a ResNet18 backbone [36] pretrained on ImageNet [40] as a feature extractor before HDC encoding, as shown in Fig. 2 and Table I. We emphasize that using a pretrained and frozen feature extractor is standard in HDC-based FL for image datasets [9], [10]. Since the feature extractor is pretrained on a different dataset (e.g., ImageNet), FedUHD has no prior knowledge of the FL workloads (e.g., CIFAR) at the start of training, ensuring a fair comparison with all baselines.

The number of local epochs (E) is set to 10 and the partition ratio (P) is 1.0 for all cases. For the dimensionality of hypervectors, we use 1,000 for the HAR dataset and 10,000 for the CIFAR-10/100 datasets following previous work [9], [37]. The neighborhood size k_n and number of global clusters J are set to 4/8/16 and 12/64/128 based on validation experiments (HAR/CIFAR10/100, respectively). We further perform sensitivity analyses on k_n and J , with the results reported in Section IV-B. For training, we use 8 NVIDIA V100 GPUs for baseline models and NVIDIA RTX 4090 for FedUHD. Training time and energy efficiency comparisons are measured on an NVIDIA RTX 4090.

B. Comparison with the State of the Art

Accuracy: Table II shows the accuracy results from FedUHD and baselines. Note that we utilize unsupervised cluster accuracy (ACC) [31], [32] which generally results in lower values compared to the accuracy observed in supervised learning. The results indicate that FedUHD consistently outperforms across various datasets and numbers of clients. These findings underscore the effectiveness of FedUHD in handling non-

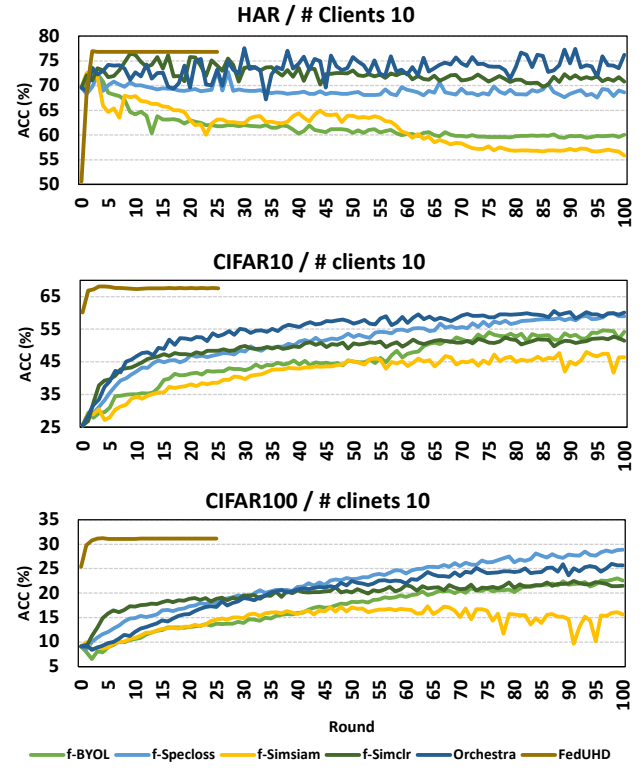


Fig. 4: Comparison of convergence rate with NN-based UFL. The x-axis is round and y-axis is accuracy.

iid data distributions, attributable to kNN-based cluster HV removal on local devices and weighted HDC aggregation on the central server. Without employing kNN-based cluster HV removal on local devices, the accuracy difference is as significant as 6.9%pt. In scenarios where the number of clients is 10, representing a case where devices have relatively abundant resources, FedUHD achieves an accuracy improvement of 0.85%, 10.58% and 7.85% in the HAR, CIFAR10 and CIFAR100 datasets, respectively. This demonstrates that FedUHD achieves comparable representation quality to the baselines on both tabular and image datasets. With 100 clients, indicating a setting where each device has limited resources, the accuracy improvement substantially increases to 22.62% and 44.88% on the CIFAR10 and CIFAR100 datasets, respectively. This notable enhancement in accuracy under the cases with 100 clients suggests FedUHD has capability to effectively manage large-scale, distributed environments, highlighting its potential for real-world applications where numerous edge devices contribute to the overall model.

Training time and energy efficiency: As illustrated in Fig. 4, one of the key advantages of FedUHD is its rapid convergence speed. In contrast to NN-based UFL, requiring intensive computations such as backpropagation for retraining in every round, FedUHD incurs significantly lower overhead by employing a single kNN operation and a limited number of epochs for k-means clustering. Another advantage of FedUHD is its ability to perform all computations in parallel enabling faster training even with limited memory resources. In contrast, training NN-based UFL models requires consideration of dependencies

TABLE II: Accuracy comparison of FedUHD with NN-based UFL: The highest accuracy is bold, second-highest accuracy is underlined.

Frameworks	HAR		CIFAR-10		CIFAR-100	
	clients = 10	clients = 100	clients = 10	clients = 100	clients = 10	clients = 100
f-BYOL [33]	60.04	54.17	35.12	22.54	11.34	
f-specloss [2]	68.6	58.99	42.30	<u>28.85</u>	15.33	
f-simsiam [34]	55.85	46.40	25.73	15.61	8.122	
f-simclr [35]	70.77	51.49	38.81	21.52	14.85	
Orchestra [6]	76.20	61.08	<u>55.27</u>	25.69	<u>18.54</u>	
FedUHD (Ours)	76.85	67.54	67.77	31.11	26.86	

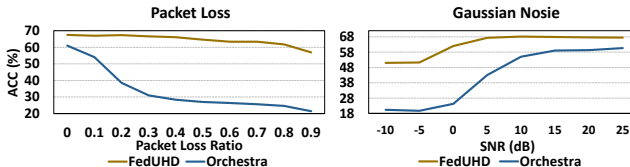


Fig. 5: Comparison of robustness with NN-based UFL [6] on CIFAR10 dataset with 10 clients.

across layers, which typically demands memory usage that is approximately three times the number of parameters required for inference [13]¹. As a result, the time required for local training is significantly shorter compared to NN-based UFL. Moreover, FedUHD converges in fewer rounds than NN-based UFL indicating that the number of communication rounds required for training FedUHD is considerably low. On average, FedUHD achieves a $87.41\times$ speedup and a $210.6\times$ improvement in energy efficiency over the state-of-the-art NN-based UFL method [6]. These results show the significant advantages of utilizing FedUHD for UFL in resource-constrained environments.

Communication cost: Fig. 4 shows that FedUHD achieves accuracy convergence in fewer rounds so that it completes training much earlier than NN-based UFL. We stop FedUHD after 25 rounds as the accuracy saturates. Additionally, FedUHD needs a lower communication cost compared to NN-based UFL in each round. In NN-based UFL, the feature extractor must be exchanged every round. In contrast, FedUHD only requires the transmission of information regarding local centroid HVs and the size of each cluster, significantly reducing the data exchanged between the server and clients each round. In detail, FedUHD needs to transfer the product of the number of clusters 12/64/128 trained on HAR/CIFAR10/100 and the dimension of each local centroid HV (1,000 for HAR and 10,000 for CIFAR10/100) with just 25 rounds. This results in $271\times/72\times/36\times$ less communication cost compared to baselines in HAR/CIFAR10/100 dataset.

Robustness: Robustness is a critical factor due to the unreliable communication encountered by edge devices. As illustrated in Fig. 5, we evaluate two different communication failure scenarios: packet loss and the addition of Gaussian noise, both of which are commonly encountered in real-world environments [10]. The results demonstrate that FedUHD exhibits superior robustness across all scenarios when compared

¹For training 1000 32×32 images in a client with 10 epochs, ResNet18 without FC layers requires 471.2 GFLOPs and 187.9 MB memory footprint with a batch size of 128, whereas FedUHD requires 2.076 GFLOPs and 40.45 MB memory footprint on average applying kNN-based cluster HV removal.

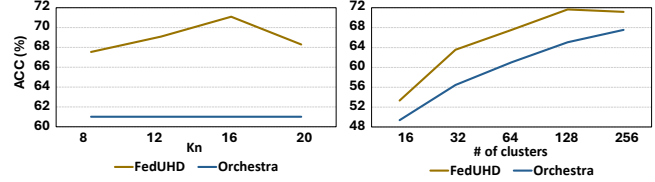


Fig. 6: Comparison of final ACC under various k_n and the number of clusters (J) on CIFAR10 dataset with 10 clients.

to Orchestra [6]. For quantitative analysis, accuracy degradation is calculated as follows:

$$\frac{(base\ accuracy) - (perturbed\ accuracy)}{base\ accuracy} * 100 \quad (3)$$

Under packet loss conditions, the accuracy degradation is 15.68% for FedUHD and 64.95% for Orchestra, while under Gaussian noise conditions, the accuracy degradation is 24.46% for FedUHD and 66.48% for Orchestra. These results show that the model of FedUHD composed of HVs exhibits greater resilience to noise compared to the state-of-the-art NN-based UFL methods [6].

Sensitivity Analysis: Fig. 6 illustrates the impact of k_n as well as the number of clusters J in FedUHD and Orchestra [6]. k_n adjusts the neighborhood size in the kNN-based HV removal phase, with $k_n = 16$ generating the best ACC. Overall, FedUHD shows robust performance with k_n in a reasonable range between 8 and 20, consistently outperforming Orchestra. The number of clusters J is a key design choice in cluster-based UFL such as FedUHD and Orchestra, when the number of ground-truth classes is not provided. As shown in Fig. 6 (right), increasing J improves ACC by allowing finer-grained clusters to align better with true labels. Notably, for the same number of global clusters, FedUHD consistently outperforms Orchestra, demonstrating the effectiveness of our design.

V. CONCLUSION

UFL has emerged as a promising decentralized learning paradigm that eliminates the need for extensive data labeling. UFL faces key challenges, including non-iid data, high computational and communication costs, and fragility to communication noise. To address these issues, we proposed FedUHD, the first UFL framework based on HDC. FedUHD introduces two key contributions: (1) a kNN-based cluster HV removal to handle non-iid data on clients, and (2) a weighted HDC aggregation to balance client data distributions on a server. Our results show that FedUHD achieves up to $173.6\times$ and $612.7\times$ better speedup and energy efficiency, respectively, up to $271\times$ lower communication costs, and 15.50% higher accuracy on average across datasets, demonstrating superior robustness

across various communication failure scenarios compared to the state-of-the-art NN-based UFL framework.

ACKNOWLEDGMENT

This work was supported in part by CoCoSys and PRISM, centers in JUMP 2.0, an SRC program sponsored by DARPA, SRC Global Research Collaboration (GRC) grants, and NSF grants #1826967, #1911095, #2003279, #2052809, #2112665, #2112167, #2100237, and #2211386.

REFERENCES

- [1] Y. Pang, Z. Ni, and X. Zhong, “Federated learning for crowd counting in smart surveillance systems,” *IEEE Internet of Things Journal*, 2023.
- [2] J. Z. HaoChen, C. Wei, A. Gaidon, and T. Ma, “Provable guarantees for self-supervised deep learning with spectral contrastive loss,” *Advances in Neural Information Processing Systems*, vol. 34, pp. 5000–5011, 2021.
- [3] W. Zhuang, X. Gan, Y. Wen, S. Zhang, and S. Yi, “Collaborative unsupervised visual representation learning from decentralized data,” in *ICCV 2021*, 2021, pp. 4892–4901.
- [4] N. Lu, Z. Wang, X. Li, G. Niu, Q. Dou, and M. Sugiyama, “Federated learning from only unlabeled data with class-conditional-sharing clients,” in *International Conference on Learning Representations*, 2022. [Online]. Available: <https://openreview.net/forum?id=WHA8009laxu>
- [5] S. Han, S. Park, F. Wu, S. Kim, C. Wu, X. Xie, and M. Cha, “Fedx: Unsupervised federated learning with cross knowledge distillation,” in *European Conference on Computer Vision*. Springer, 2022, pp. 691–707.
- [6] E. S. Lubana, C. I. Tang, F. Kawsar, R. P. Dick, and A. Mathur, “Orchestra: Unsupervised federated learning via globally consistent clustering,” in *International Conference on Machine Learning*, 2022. [Online]. Available: <https://api.semanticscholar.org/CorpusID:248987363>
- [7] A. Anwar, “Difference between alexnet, vggnet, resnet, and inception,” <https://towardsdatascience.com/the-w3h-of-alexnet-vggnet-resnet-and-inception-7baaaecc96>, 2019, accessed: 2024-08-12.
- [8] H. Ye, L. Liang, and G. Y. Li, “Decentralized federated learning with unreliable communications,” *IEEE journal of selected topics in signal processing*, vol. 16, no. 3, pp. 487–500, 2022.
- [9] Q. Zhao, K. Lee, J. Liu, M. Huzaifa, X. Yu, and T. Rosing, “Fedhd: Federated learning with hyperdimensional computing,” in *Proceedings of the 28th Annual International Conference on Mobile Computing And Networking*, ser. MobiCom ’22. New York, NY, USA: Association for Computing Machinery, 2022, p. 791–793. [Online]. Available: <https://doi.org/10.1145/3495243.3558757>
- [10] R. Chandrasekaran, K. Ergun, J. Lee, D. Nanjunda, J. Kang, and T. Rosing, “Fhdnn: Communication efficient and robust federated learning for aiot networks,” in *Proceedings of the 59th ACM/IEEE Design Automation Conference*, ser. DAC ’22. New York, NY, USA: Association for Computing Machinery, 2022, p. 37–42. [Online]. Available: <https://doi.org/10.1145/3489517.3530394>
- [11] J. Kang, Y. H. Lee, M. Zhou, W. Xu, and T. Rosing, “Hyghd: Hyperdimensional hypergraph learning,” in *2024 Design, Automation & Test in Europe Conference & Exhibition (DATE)*. IEEE, 2024, pp. 1–6.
- [12] L. Ge and K. K. Parhi, “Classification using hyperdimensional computing: A review,” *IEEE Circuits and Systems Magazine*, vol. 20, no. 2, pp. 30–47, 2020.
- [13] I. Gim and J. Ko, “Memory-efficient dnn training on mobile devices,” in *Proceedings of the 20th Annual International Conference on Mobile Systems, Applications and Services*, ser. MobiSys ’22. New York, NY, USA: Association for Computing Machinery, 2022, p. 464–476. [Online]. Available: <https://doi.org/10.1145/3498361.3539765>
- [14] A. Thomas, S. Dasgupta, and T. Rosing, “A theoretical perspective on hyperdimensional computing,” *Journal of Artificial Intelligence Research*, vol. 72, pp. 215–249, 2021.
- [15] P. Kanerva, “Hyperdimensional computing: An introduction to computing in distributed representation with high-dimensional random vectors,” *Cognitive computation*, vol. 1, pp. 139–159, 2009.
- [16] M. Imani, Z. Zou, S. Bosch, S. A. Rao, S. Salamat, V. Kumar, Y. Kim, and T. Rosing, “Revisiting hyperdimensional learning for fpga and low-power architectures,” in *2021 IEEE International Symposium on High-Performance Computer Architecture (HPCA)*. IEEE, 2021, pp. 221–234.
- [17] S. Salamat, M. Imani, B. Khaleghi, and T. Rosing, “F5-hd: Fast flexible fpga-based framework for refreshing hyperdimensional computing,” in *Proceedings of the 2019 ACM/SIGDA International Symposium on Field-Programmable Gate Arrays*, 2019, pp. 53–62.
- [18] I. G. Moreno, X. Yu, and T. Rosing, “Kalmahd: Robust on-device time series forecasting with hyperdimensional computing,” in *2024 29th Asia and South Pacific Design Automation Conference (ASP-DAC)*. IEEE, 2024, pp. 710–715.
- [19] B. Khaleghi, H. Xu, J. Morris, and T. Š. Rosing, “tiny-hd: Ultra-efficient hyperdimensional computing engine for iot applications,” in *2021 Design, Automation & Test in Europe Conference & Exhibition (DATE)*. IEEE, 2021, pp. 408–413.
- [20] D. Rachkovskij, “Formation of similarity-reflecting binary vectors with random binary projections,” *Cybernetics and Systems Analysis*, vol. 51, pp. 313–323, 2015.
- [21] A. Rahimi and B. Recht, “Random features for large-scale kernel machines,” *Advances in neural information processing systems*, vol. 20, 2007.
- [22] F. Rosenblatt, “The perceptron: a probabilistic model for information storage and organization in the brain.” *Psychological review*, vol. 65, no. 6, p. 386, 1958.
- [23] C.-Y. Hsieh, Y.-C. Chuang, and A.-Y. A. Wu, “Fl-hdc: Hyperdimensional computing design for the application of federated learning,” in *2021 IEEE 3rd International Conference on Artificial Intelligence Circuits and Systems (AICAS)*, 2021, pp. 1–5.
- [24] N. Zeulin, O. Galinina, N. Himayat, and S. Andreev, “Resource-efficient federated hyperdimensional computing,” *arXiv preprint arXiv:2306.01339*, 2023.
- [25] A. Dutta, S. Gupta, B. Khaleghi, R. Chandrasekaran, W. Xu, and T. Rosing, “Hdnn-pim: Efficient in memory design of hyperdimensional computing with feature extraction,” in *Proceedings of the Great Lakes Symposium on VLSI 2022*, 2022, pp. 281–286.
- [26] M.-F. F. Balcan, S. Ehrlich, and Y. Liang, “Distributed k -means and k -median clustering on general topologies,” *Advances in neural information processing systems*, vol. 26, 2013.
- [27] B. McMahan, E. Moore, D. Ramage, S. Hampson, and B. A. y Arcas, “Communication-efficient learning of deep networks from decentralized data,” in *Artificial intelligence and statistics*. PMLR, 2017, pp. 1273–1282.
- [28] K. Kerdprasop, N. Kerdprasop, and P. Sattayatham, “Weighted k -means for density-biased clustering,” in *International conference on data warehousing and knowledge discovery*. Springer, 2005, pp. 488–497.
- [29] J. Reyes-Ortiz, D. Anguita, A. Ghio, L. Oneto, and X. Parra, “Human Activity Recognition Using Smartphones,” UCI Machine Learning Repository, 2013, DOI: <https://doi.org/10.24432/C54S4K>.
- [30] A. Krizhevsky, G. Hinton *et al.*, “Learning multiple layers of features from tiny images,” 2009.
- [31] J. Xie, R. Girshick, and A. Farhadi, “Unsupervised deep embedding for clustering analysis,” in *International conference on machine learning*. PMLR, 2016, pp. 478–487.
- [32] X. Yu, A. Thomas, I. G. Moreno, L. Gutierrez, and T. Rosing, “Lifelong intelligence beyond the edge using hyperdimensional computing,” *arXiv preprint arXiv:2403.04759*, 2024.
- [33] J.-B. Grill, F. Strub, F. Altché, C. Tallec, P. Richemond, E. Buchatskaya, C. Doersch, B. Avila Pires, Z. Guo, M. Gheshlaghi Azar *et al.*, “Bootstrap your own latent-a new approach to self-supervised learning,” *Advances in neural information processing systems*, vol. 33, pp. 21 271–21 284, 2020.
- [34] X. Chen and K. He, “Exploring simple siamese representation learning,” in *Proceedings of the IEEE/CVF conference on computer vision and pattern recognition*, 2021, pp. 15 750–15 758.
- [35] T. Chen, S. Kornblith, M. Norouzi, and G. Hinton, “A simple framework for contrastive learning of visual representations,” in *International conference on machine learning*. PMLR, 2020, pp. 1597–1607.
- [36] K. He, X. Zhang, S. Ren, and J. Sun, “Deep residual learning for image recognition,” in *Proceedings of the IEEE conference on computer vision and pattern recognition*, 2016, pp. 770–778.
- [37] Y. Kim, M. Imani, and T. S. Rosing, “Efficient human activity recognition using hyperdimensional computing,” in *Proceedings of the 8th International Conference on the Internet of Things*, 2018, pp. 1–6.
- [38] S. Imambi, K. B. Prakash, and G. Kanagachidambaresan, “Pytorch,” *Programming with TensorFlow: solution for edge computing applications*, pp. 87–104, 2021.

- [39] S. Marcel and Y. Rodriguez, “Torchvision the machine-vision package of torch,” in *Proceedings of the 18th ACM international conference on Multimedia*, 2010, pp. 1485–1488.
- [40] O. Russakovsky, J. Deng, H. Su, J. Krause, S. Satheesh, S. Ma, Z. Huang, A. Karpathy, A. Khosla, M. Bernstein *et al.*, “Imagenet large scale visual recognition challenge,” *International journal of computer vision*, vol. 115, pp. 211–252, 2015.